

Reentrant ferromagnetism in a class of diluted magnetic semiconductors

M. J. Calderón^{1,2} and S. Das Sarma¹

¹*Condensed Matter Theory Center, Department of Physics, University of Maryland, College Park, Maryland 20742-4111, USA*

²*Instituto de Ciencia de Materiales de Madrid (CSIC), Cantoblanco, 28049 Madrid, Spain*

(Received 14 November 2006; revised manuscript received 11 April 2007; published 14 June 2007)

Considering a general situation where a semiconductor is doped by magnetic impurities leading to a carrier-induced ferromagnetic exchange coupling between the impurity moments, we show theoretically the possible generic existence of three ferromagnetic transition temperatures $T_1 > T_2 > T_3$, with two distinct ferromagnetic regimes existing for $T_1 > T > T_2$ and $T < T_3$. Such an intriguing reentrant ferromagnetism, with a paramagnetic phase ($T_2 > T > T_3$) between two ferromagnetic phases, arises from a subtle competition between indirect exchange induced by thermally activated carriers in an otherwise empty conduction band versus the exchange coupling existing in the impurity band due to the bound carriers themselves. We comment on the possibility of observing such a reentrance phenomenon in diluted magnetic semiconductors and magnetic oxides.

DOI: [10.1103/PhysRevB.75.235203](https://doi.org/10.1103/PhysRevB.75.235203)

PACS number(s): 75.10.-b, 75.30.Hx, 75.50.Pp

I. INTRODUCTION

The large class of materials comprised of diluted magnetic semiconductors and magnetic oxides (DMSs) has been widely studied in the recent years for their potential in spintronic applications as well as for the fundamental physics of carrier-mediated ferromagnetism in semiconductors. They have ferromagnetic (FM) critical temperatures T_C ranging from below [e.g. (Ga,Mn)As] (Ref. 1) to above room temperature (e.g., doped magnetic oxides as TiO_2),² and some others never show long-range FM order (e.g., most Mn-doped II-VI semiconductor alloys are spin glasses).³ FM is usually ascribed to carrier-mediated mechanisms and depends on many different parameters [e.g., carrier density n_c , magnetic impurity density n_i , magnetic coupling between the ion moment and the electron (or hole) spins J , and details of disorder] which vary greatly from system to system and sometimes from sample to sample. When the concentration of magnetic impurities is larger than a few percent, direct exchange (i.e., not carrier mediated) can also be significant. This exchange is antiferromagnetic in many cases, like the Mn-doped III-V⁴ and II-VI⁵ semiconductors, and ferromagnetic in others, like Co-doped TiO_2 .⁶

The accepted effective theoretical models⁷⁻¹¹ for FM in DMSs can be roughly divided into two broad categories depending on whether the carriers mediating the FM interaction between the magnetic impurities are itinerant free carriers (i.e., holes in the valence band or electrons in the conduction band) or localized (or bound) carriers (in an impurity band, for example). For the itinerant free carrier case—e.g., $\text{Ga}_{1-x}\text{Mn}_x\text{As}$ in the optimally doped ($x \approx 0.05$) situation with the nominally high T_C (~ 100 – 170 K)—the effective magnetic interaction producing FM is thought to be of the Ruderman-Kittel-Kasuya-Yosida (RKKY) type,⁷⁻¹³ leading to a mean-field FM transition by virtue of there being many more effective impurity magnetic moments than free carriers. Such RKKY carrier-mediated mean-field FM seems to describe well^{7,10,11} the optimally doped (Ga,Mn)As regime. For the localized case, where disorder should play an important role, the FM transition is thought to be caused by the temperature-driven magnetic percolation transition of

bound magnetic polarons (BMPs),^{14,15} objects where one localized carrier is magnetically strongly correlated with a few neighboring magnetic impurities through the local exchange interaction. An example of such BMP percolation-induced FM is thought to be the localized impurity-band $\text{Ge}_{1-x}\text{Mn}_x$ DMS system.¹⁶ Typically, the RKKY (BMP percolation) ferromagnetic T_C is relatively high (low).

In this article, we introduce an RKKY-like mechanism, which we dub “activated” RKKY, mediated by *thermally excited free carriers*.¹⁷ In the low-temperature regime, where thermal activation is exponentially suppressed, this mechanism alone would give paramagnetism, whereas long-range ferromagnetism would appear as the temperature increases (an example of “order-by-disorder” phenomena). At higher temperature, the system will of course be paramagnetic again, leading to a reentrant paramagnetism scenario: a ferromagnetic phase between two paramagnetic phases at higher and lower temperatures. Furthermore, the activated RKKY mechanism could coexist at low temperature with BMP percolation in the impurity band, a mechanism which does not require the existence of free carriers to produce a FM phase. We analyze theoretically such an interesting multimechanism DMS situation using simple physical models and show that it may be generically possible for DMS materials to have reentrant ferromagnetism with a paramagnetic state sandwiched between the high-temperature activated RKKY-type and the low-temperature BMP percolation-type FM.

In Sec. II below we introduce the model and present the phase diagrams corresponding to the activated RKKY alone (Sec. II A) and to the competition of the activated RKKY and BMP percolation (Sec. II B). In Sec. III we discuss the conditions to observe reentrance phenomena in diluted magnetic semiconductors. We conclude in Sec. IV.

II. MODEL

The system considered is a localized impurity-band system which is insulating at $T=0$. In this scenario, the density of band carriers is a function of temperature T and activation energy Δ , and can be written

$$n_c(T, \Delta) = n_{c0} \exp(-\Delta/k_B T). \quad (1)$$

As a consequence, the RKKY-like mechanism is inefficient at low temperature (typically for $T < \Delta$) when the free carrier density is too low, while the activated carriers can mediate FM at higher temperatures. Therefore, this activated RKKY mechanism leads, by itself, to a FM phase between two disordered phases at high $T > T_1$ and low $T < T_2$ temperatures (*reentrant paramagnetism*). At low temperature, other mechanisms not requiring free carriers (e.g., magnetic polaron percolation) could come into play, producing a further magnetic transition with critical temperature T_3 . When $T_3 < T_2$ there are two distinct ferromagnetic phases and the system exhibits *reentrant ferromagnetism*. The inclusion of the band spin splitting (which can be different for the localized and extended states) and the nontrivial dependence of Δ on temperature and magnetization,¹⁸ which we are neglecting in Eq. (1), are not expected to produce qualitative changes to our conclusions—i.e., the possible existence of reentrance phenomena in magnetic semiconductors.

The Hamiltonian of the exchange interaction between magnetic impurities and the carriers is

$$H = \sum_i J a_0^3 \mathbf{S}_i \cdot \mathbf{s}(\mathbf{R}_i), \quad (2)$$

where J is the local exchange coupling between the impurity spin \mathbf{S}_i located at \mathbf{R}_i and the carrier spin density $\mathbf{s}(\mathbf{r})$, and a_0^3 is the unit cell volume.

A. Reentrant paramagnetism: An example of order-by-disorder phenomena

We first discuss the case of an intrinsic semiconductor with magnetic impurities which do not contribute carriers (therefore, there exists no impurity band where BMPs could form). In this case, the RKKY mechanism can only be mediated by carriers thermally activated from the valence to the conduction band. Another mechanism that could play a role in this intrinsic case is the Bloembergen-Rowland mechanism¹⁹ mediated by virtual electron excitations across the band gap. This mechanism was considered in the context of II-VI DMS³ and was finally dismissed as being too weak compared to superexchange.⁵ Therefore, we do not further include this mechanism in our discussion.

We now consider this activated RKKY mechanism within a mean-field theory in the limit of nondegenerate carriers. Unlike more exact *ab initio* calculations, mean-field theory captures correctly the competition between entropy and energy and works well on the small energy scale relevant for activated carriers. In the activated carrier scenario we are studying, the Fermi energy is smaller than the temperature, and hence the limit of nondegenerate carriers is appropriate. Within mean-field theory, the impurity spins act upon the carrier spins as an effective magnetic field $\propto J a_0^3 n_i \langle S_z \rangle$ while the carrier spins act upon the impurity spins with an effective field $\propto J a_0^3 n_c \langle s_z \rangle$.¹⁷ As a result, the magnetization of the magnetic impurities $\langle S_z \rangle / S$ is calculated self-consistently, giving

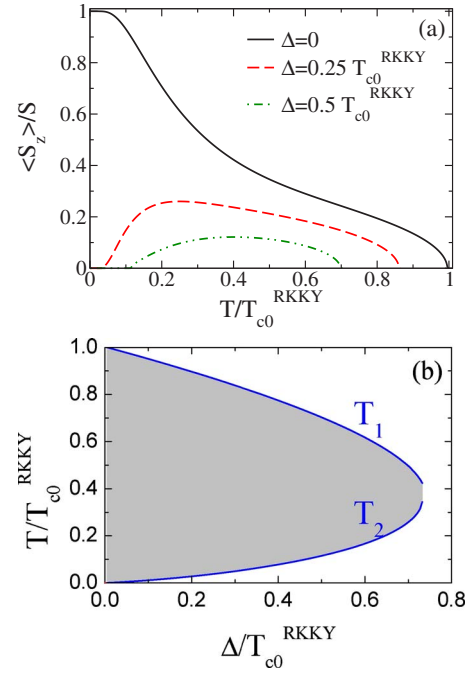


FIG. 1. (Color online) (a) Impurity magnetization $\langle S_z \rangle / S$ corresponding to the reentrant paramagnetism given by the activated RKKY model, Eq. (3), for different values of the carrier activation energy Δ . The parameters used are $n_{c0} = 3 \times 10^{20} \text{ cm}^{-3}$, $n_i = 3 \times 10^{21} \text{ cm}^{-3}$, and $J = 1 \text{ eV}$. (b) The phase diagram (with two critical temperatures T_1 and T_2) of the activated RKKY model given by Eq. (3). The shaded area is ferromagnetic while the white area is paramagnetic. T and Δ are in units of $T_{c0}^{\text{RKKY}} \equiv T_1(\Delta=0)$.

$$\frac{\langle S_z \rangle}{S} = B_s \left[\frac{J a_0^3 n_c(T, \Delta)}{k_B T} s B_s \left(\frac{J a_0^3 n_i \langle S_z \rangle}{k_B T} \right) \right], \quad (3)$$

where $B_s(y)$ is the Brillouin function. The magnetization is plotted in Fig. 1(a) for three different values of Δ . The $\Delta=0$ curve has a nonstandard concave shape as expected for a low density of carriers.¹² The critical temperatures are given by the points at which the magnetic susceptibility diverges. The susceptibility is essentially that of the magnetic impurities, as usually $n_c \ll n_i$ due to carrier compensation, and in the paramagnetic regions is given by $\chi(T) \equiv n_i \partial(g_i \mu_B \langle S_z \rangle) / \partial B$. For $\Delta=0$, there is only one critical temperature given by

$$T_{c0}^{\text{RKKY}} = \frac{1}{3} J a_0^3 \sqrt{n_{c0} n_i} \sqrt{(S+1)(s+1)}. \quad (4)$$

For $\Delta \neq 0$, the model gives two critical temperatures T_1 and T_2 , shown in Fig. 1(b): at low temperature, n_c gets exponentially suppressed and the localized moments are independent of each other (the system is paramagnetic); as T increases, the band gets populated and the carrier-mediated FM kicks in at T_2 , which increases with Δ . At even higher T , thermal disorder produces the standard ferro-to-paramagnetic transition with critical temperature T_1 , which decreases as Δ increases, due to the reduction of carrier density in the band. In summary, the system shows a ferromagnetic phase between two paramagnetic phases (*reentrant paramagnetism*). For any set of parameters, the T_1 and T_2 curves meet at Δ

$\approx 0.73T_{c0}^{\text{RKKY}}$ and, for $\Delta > 0.73T_{c0}^{\text{RKKY}}$, the density of carriers is always too low to mediate FM, so the activated RKKY model gives paramagnetism at all temperatures. Note that the curves for different parameters scale exactly with $T_{c0}^{\text{RKKY}} \equiv T_1(\Delta=0)$.

B. Competition of activated RKKY and polaron percolation: Reentrant ferromagnetism

We consider now the case in which there is an impurity band. The carriers in the impurity band can come from magnetic impurities acting as dopants, like in the III-V semiconductors, or from other dopants, like the oxygen vacancies which act as shallow donors in the magnetic oxides. We assume that at $T=0$ the conduction (or valence) band is empty, so all the free carriers in the band are produced by thermal activation from the impurity band. At low temperature, the carriers in the impurity band can be strongly localized and mediate FM through the formation of BMPs which grow as the temperature lowers, finally overlapping in clusters and producing a FM transition at percolation.¹⁴ In our model of thermally activated carriers, the density of carriers in the impurity band is

$$n_c^*(T, \Delta) = n_{c0} - n_c = n_{c0}[1 - \exp(-\Delta/k_B T)], \quad (5)$$

where n_c is the density of carriers in the valence or conduction band defined in Eq. (1). Δ is the smallest energy gap for electron excitations, which in this case is given by the activation energy of a carrier at the impurity level. The critical temperature in the BMP percolation model is given by¹⁴

$$T_c^{\text{perc}} = sSJ \left(\frac{a_0}{a_B} \right)^3 (a_B^3 n_c^*)^{1/3} \sqrt{\frac{n_i}{n_c^*}} e^{-0.86/(a_B^3 n_c^*)^{1/3}}, \quad (6)$$

where a_B is the carrier localization radius and n_c^* is the carrier density at T_c^{perc} . Equation (6) is valid in the low-carrier-density limit $a_B^3 n_c^* \ll 1$. As the density of carriers involved in polaron formation n_c^* increases with Δ , T_c^{perc} also increases, saturating for large values of Δ , when $n_c^* \approx n_{c0}$, as shown in Fig. 2 (solid line). The value of T_c^{perc} is mainly dominated by the value of $a_B^3 n_c^*$, on which it depends exponentially. Another mechanism that could arise when there are no free carriers is the Bloembergen-Rowland-type mechanism proposed in Ref. 20 in the context of Mn-doped III-V semiconductors, where virtual carrier excitations between the impurity levels and the itinerant band mediate ferromagnetism. We do not expect, however, this mechanism to be stronger than the BMP percolation, and therefore, it does not affect our conclusions.

In Fig. 2 we show two typical phase diagrams resulting from the interplay of the activated RKKY and BMP percolation models. The parameters chosen here are representative of real systems. We have fixed the magnetic impurity concentration to $x=0.1$, $J=1$ eV, and $S=1$. The other two main parameters left are n_{c0} and a_B . n_{c0} is chosen so that $n_{c0}/n_i \leq 0.1$, as is usually found in DMS systems due to strong carrier compensation. Finally, a_B is chosen to fulfill the applicability conditions of Eq. (6). There are two qualitatively different phase diagrams that can occur depending on the

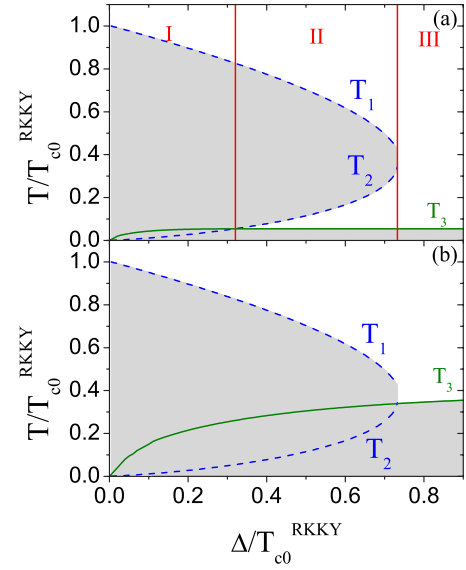


FIG. 2. (Color online) Phase diagrams for the activated RKKY-BMP percolation combined model in two typical cases. The dashed lines represent the two critical temperatures of the activated RKKY model, Eq. (3). The solid line is the critical temperature in the bound magnetic polaron percolation model given by Eq. (6), $T_3 \equiv T_c^{\text{perc}}$. The shaded areas are the ferromagnetic phases and the white ones are paramagnetic. The parameters used are $n_i=3 \times 10^{21} \text{ cm}^{-3}$, $J=1$ eV, $a_0=3.23 \text{ \AA}$ and (a) $n_{c0}=3 \times 10^{19} \text{ cm}^{-3}$, $a_B=4 \text{ \AA}$ ($a_B^3 n_{c0} \approx 0.002$), (b) $n_{c0}=1 \times 10^{20} \text{ cm}^{-3}$, $a_B=5 \text{ \AA}$ ($a_B^3 n_{c0} \approx 0.0125$). T and Δ are in units of $T_{c0}^{\text{RKKY}} \equiv T_1(\Delta=0)$. Reentrant ferromagnetism shows in region II of (a); see text for discussion.

value of $a_B^3 n_{c0}$. For the lowest values of $a_B^3 n_{c0}$, $T_3 \equiv T_c^{\text{perc}}$ is relatively small, and we get the novel scenario depicted in Fig. 2(a): in region I, corresponding to $\Delta/T_{c0}^{\text{RKKY}} \leq 0.32$ for the particular parameter values chosen in this figure, the system is FM with critical temperature T_1 ; in region III, with $\Delta/T_{c0}^{\text{RKKY}} \geq 0.73$ for any set of parameters, the system is FM with $T_c=T_3$; finally, in region II, which corresponds to intermediate values of Δ ($0.32 \leq \Delta/T_{c0}^{\text{RKKY}} \leq 0.73$ for our parameters), $T_3 < T_2$ and the system shows reentrant ferromagnetism with three distinct critical temperatures T_1 , T_2 , and T_3 . For larger values of $a_B^3 n_{c0}$ (but still $\ll 1$), as in Fig. 2(b), $T_3 > T_2$ for all values of Δ and the system is ferromagnetic for $T < \max(T_1, T_3)$. When $T_3 > T_2$ [as in region I of Fig. 2(a) and for $\Delta/T_{c0}^{\text{RKKY}} \leq 0.73$ in Fig. 2(b)], the ferromagnetism would be caused by BMP percolation at low temperature and would turn *continuously* into an activated RKKY mechanism at higher temperature, therefore showing only one (the highest) critical temperature.

Note that we have assumed the local exchange J to be the same in the impurity and the conduction bands. Generally speaking, the local exchange parameters could be different in Eqs. (3) and (6) and could lead to the two extreme cases of a phase diagram dominated by the activated RKKY mechanism ($T_3=0$, illustrated in Fig. 1) or by the BMP mechanism ($T_3 \gg T_1, T_2$).

III. DISCUSSION

Although our theoretical analysis, being physically motivated, is formally correct, it relies on simple models and

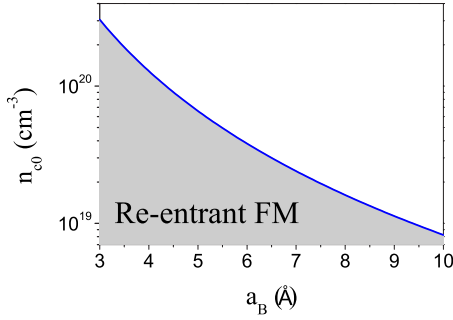


FIG. 3. (Color online) The shaded area gives the values of a_B and n_{c0} compatible with the reentrant ferromagnetism behavior illustrated in region II of Fig. 2(a). The curve is given by $a_B^3 n_{c0} = 0.00824$ (see Sec. III for details).

depends on several nonaccurately known parameters. Therefore, it could be possible that our predicted reentrant paramagnetism (Sec. II A) and reentrant ferromagnetism (Sec. II B) behaviors are outside the parameters range of existing materials and, perhaps, at too low temperature. However, we can make a qualitative discussion about the observability of reentrance in DMS materials considering the three general conditions that should be met: (i) at $T=0$ there should be no carriers in the conduction (or valence) band, so all the carriers mediating RKKY come from thermal activation; (ii) for the scenario illustrated in Fig. 2(a) to occur we need to fulfill the condition $T_c^{\text{perc}}(n_{c0}) < T_2^{\text{max}} \approx 0.3 \times T_c^{\text{RKKY}}(n_{c0})$; and (iii) we also have to ensure that the system is in region II in Fig. 2(a) to actually observe reentrant ferromagnetism. If, for some reason, the BMP mechanism were inactive ($T_3=0$), reentrant ferromagnetism would be replaced by the reentrant paramagnetism of Fig. 1.

Condition (i) basically implies that the system has to have activatedlike resistivity (decreasing as T increases) limiting the suitable systems to those with so-called “insulating behavior,”—for example, very lightly doped (Ga,Mn)As, (In,Mn)As, and magnetic oxides. Condition (ii) puts restrictions on the relative values of a_B and n_{c0} . The equation in (ii) is independent of J and n_i and reduces to the inequality $a_B^3 n_{c0} < 0.00824$ for $S=1$. This result is illustrated in Fig. 3 where the curve is given by the maximum allowed value of the product $a_B^3 n_{c0}$. Below this curve we get the scenario in Fig. 2(a) while the scenario in Fig. 2(b) occurs for a_B and n_{c0} values above the curve. The carrier confinement radius is given by $a_B = \epsilon(m/m^*)a$ where $a=0.52 \text{ \AA}$, ϵ is the semiconductor dielectric constant, and m^* is the polaron mass (usually $m^*/m > 1$). For diluted magnetic semiconductors and magnetic oxides we generally expect $3 \text{ \AA} < a_B < 10 \text{ \AA}$. Hence, as shown in Fig. 3, which is the important materials phase diagram to keep in mind in searching for a suitable system to observe our predicted reentrance, we need to keep a relatively low density of carriers, which is well within experimentally achievable values.

Condition (iii) can be fulfilled, in general terms, when Δ is comparable to T_c . This rules out $\text{Ga}_{1-x}\text{Mn}_x\text{As}$, with $\Delta/T_c \sim 10$ ($T_c \sim 100 \text{ K}$ and $\Delta \approx 110 \text{ meV}$),²¹ which would rather be in region III (for very-low-carrier-density samples). Probably this is also the case of $\text{In}_{1-x}\text{Mn}_x\text{As}$ with $T_c \sim 50 \text{ K}$, al-

though it has a much lower activation energy (see, for example, Fig. 2 in Ref. 22). The most likely candidate for observing our predicted reentrant ferromagnetism is possibly a doped magnetic oxide material—e.g., $\text{Ti}_{1-x}\text{Co}_x\text{O}_2$ (with $30 \text{ meV} < \Delta < 70 \text{ meV}$ ²³ and very similar critical temperatures $T_c \sim 700 \text{ K}$), which is an insulator at low temperature, but exhibits essentially T -independent Drude transport behavior, due to thermally activated carriers, at room temperature or above. In such a system, it is quite possible that the high-temperature FM is mediated by thermally activated carriers, whereas at low temperature a BMP percolation FM takes over¹⁵ as in region I of Fig. 2(a).²⁴ It is then possible that a small modification of the system parameters (e.g., the activation energy Δ which varies from sample to sample) can put the system in the reentrant ferromagnetism region II of Fig. 2(a).

We have neglected the direct exchange (i.e., not carrier mediated) interaction between the magnetic impurities, which is short ranged and could also play a role, particularly when the density of impurities n_i is large. In many cases the direct exchange is antiferromagnetic and could completely destroy the lower FM phase,²⁵ leading to a spin-glass phase. These spin-glass low- T phases have been observed in II-VI DMSs,³ and (Ga,Mn)N,²⁶ in samples that never show FM order (they are very insulating). In principle, therefore, direct antiferromagnetic exchange between the magnetic dopant impurities could compete with (or even suppress) our predicted low- T reentrant ferromagnetic phase, but the origin of this direct exchange being completely different from the carrier-mediated mechanisms producing the reentrant ferromagnetism behavior itself, we find it difficult to believe that such a suppression of reentrance can be generic. On the other hand, in some of the magnetic oxides the direct exchange between the magnetic ions is ferromagnetic^{6,27} and, still, a suppression of magnetization at low temperature in zero-field-cooled curves has been reported in the magnetic oxide V-doped ZnO and (possibly) other magnetic oxides.²⁸ This could be a signature of the order-by-disorder mechanism we describe if the bound magnetic percolation mechanism were inactive in these systems (Sec. II A). We suggest detailed T -dependent magnetization studies in the shaded region of our Fig. 3 to search for our predicted reentrant ferromagnetism behavior which may have been already observed experimentally though not correctly identified.

IV. CONCLUSION

We have considered, using physically motivated effective models of ferromagnetism in diluted magnetic semiconductor materials, the intriguing possibility of generic reentrant ferromagnetism in an insulating class of diluted magnetic semiconductor systems. The models we use are considered to be successful minimal carrier-mediated models^{7–11} for understanding ferromagnetic behavior and predicting ferromagnetic critical temperatures in itinerant and localized diluted magnetic semiconductor materials. The ideas in this work have been to point out (i) the possible occurrence of a high-temperature effective ferromagnetism mediated by thermally excited carriers with a low-temperature disordered paramag-

netic phase (reentrant paramagnetism mediated by an activated RKKY mechanism—an example of order-by-disorder phenomena) and (ii) the possible coexistence of this activated RKKY with ferromagnetism mediated by localized bound carriers in an impurity band through the polaron percolation mechanism at low temperature, where thermal activation of carriers is exponentially suppressed, leading to reentrant ferromagnetism (a paramagnetic phase sandwiched between two ferromagnetic phases). More experimental

work in diluted magnetic semiconductor materials is needed to confirm the existence of such reentrance phenomena, but they should exist on firm theoretical grounds.

ACKNOWLEDGMENTS

This work was supported by the NSF and the NRI SWAN program. M.J.C. also acknowledges support from Programa Ramón y Cajal (MEC-Spain).

-
- ¹H. Ohno, A. Shen, F. Matsukura, A. Oiwa, A. Endo, S. Katsumoto, and Y. Iye, *Appl. Phys. Lett.* **69**, 363 (1996).
²Y. Matsumoto, M. Murakami, T. Shono, T. Hasegawa, T. Fukumura, M. Kawasaki, P. Ahmet, T. Chikyow, S. Koshihara, and H. Koinuma, *Science* **291**, 854 (2001).
³J. Furdyna, *J. Appl. Phys.* **64**, R29 (1988).
⁴S. von Molnar, H. Munekata, H. Ohno, and L. L. Chang, *J. Magn. Mater.* **93**, 356 (1991).
⁵B. E. Larson, K. C. Hass, H. Ehrenreich, and A. E. Carlsson, *Phys. Rev. B* **37**, 4137 (1988).
⁶R. Janisch and N. A. Spaldin, *Phys. Rev. B* **73**, 035201 (2006).
⁷T. Dietl, H. Ohno, F. Matsukura, J. Cibert, and D. Ferrand, *Science* **287**, 1019 (2000).
⁸S. Das Sarma, E. H. Hwang, and A. Kaminski, *Solid State Commun.* **127**, 99 (2003).
⁹C. Timm, *J. Phys.: Condens. Matter* **15**, R1865 (2003).
¹⁰A. MacDonald, P. Schiffer, and N. Samarth, *Nat. Mater.* **4**, 195 (2005).
¹¹T. Jungwirth, J. Sinova, J. Masek, J. Kucera, and A. H. MacDonald, *Rev. Mod. Phys.* **78**, 809 (2006).
¹²S. Das Sarma, E. H. Hwang, and A. Kaminski, *Phys. Rev. B* **67**, 155201 (2003).
¹³D. J. Priour, E. H. Hwang, and S. Das Sarma, *Phys. Rev. Lett.* **95**, 037201 (2005).
¹⁴A. Kaminski and S. Das Sarma, *Phys. Rev. Lett.* **88**, 247202 (2002).
¹⁵J. M. D. Coey, M. Venkatesan, and C. B. Fitzgerald, *Nat. Mater.* **4**, 173 (2005).
¹⁶A. P. Li, J. F. Wendelken, J. Shen, L. C. Feldman, J. R. Thompson, and H. H. Weitering, *Phys. Rev. B* **72**, 195205 (2005).
¹⁷E. A. Pashitskii and S. M. Ryabchenko, *Sov. Phys. Solid State* **21**, 322 (1979).
¹⁸J. Jaroszynski and T. Dietl, *Solid State Commun.* **55**, 491 (1985).
¹⁹N. Bloembergen and T. J. Rowland, *Phys. Rev.* **97**, 1679 (1955).
²⁰V. I. Litvinov and V. K. Dugaev, *Phys. Rev. Lett.* **86**, 5593 (2001).
²¹W. Schairer and M. Schmidt, *Phys. Rev. B* **10**, 2501 (1974).
²²T. Dietl, *Semicond. Sci. Technol.* **17**, 377 (2002).
²³S. R. Shinde *et al.* (unpublished).
²⁴M. J. Calderón and S. Das Sarma, arXiv:cond-mat/0603182, *Ann. Phys. (N.Y.)* (to be published).
²⁵A. Kaminski, V. M. Galitski, and S. Das Sarma, *Phys. Rev. B* **70**, 115216 (2004).
²⁶S. Dhar, O. Brandt, A. Trampert, K. J. Friedland, Y. J. Sun, and K. H. Ploog, *Phys. Rev. B* **67**, 165205 (2003).
²⁷R. Janisch, P. Gopal, and N. A. Spaldin, *J. Phys.: Condens. Matter* **17**, R657 (2005).
²⁸N. Hong, J. Sakai, and A. Hassini, *J. Phys.: Condens. Matter* **17**, 199 (2005).